

## DFT studies of intramolecular double proton transfer of 3,6-dihydro-3,6-diimino(silane or pyridine)-2,5-diamine

Hasan Tahermansouri\* & Lida Farhan

Department of Chemistry, Ayatollah Amoli Branch, Islamic Azad University, Amol, Iran

Email: h.tahermansouri@iauamol.ac.ir/tahermansouri@yahoo.com

Received 12 November 2015; revised and accepted 26 April 2016

Intramolecular double proton transfer of 3,6-dihydro-3,6-diiminosilane-2,5-diamine (A) and 3,6-dihydro-3,6-diiminopyridine-2,5-diamine (B) at DFT (B3LYP) level of theory has been investigated. Two mechanisms, stepwise ( $TS_1$ ) and concerted ( $TS_2$ ), are proposed for the process of proton transfer. The stepwise mechanism itself includes two pathways, the pathway (1) and pathway (2), which involve the resonance forms from side of N-C-C-C-N and N-C-X-C-N atoms (X = Si-H or N), respectively. These results show that for both the compounds the process of proton transfer is through the stepwise mechanism. The results indicate that in the case of compound (A) the process is through pathway (1), while for compound (B) the pathways (1) and (2) were almost similar to each other. In addition, aromaticity of the two compounds has been evaluated based on the nucleus independent chemical shift values to predict dominant resonance structures and the charge distributions in the ring.

**Keywords:** Theoretical chemistry, Density functional calculations, Proton transfer, Intramolecular proton transfer, Double proton transfer, Aromaticity

Proton transfers are important processes in many chemical and biological systems<sup>1-3</sup>. Several theoretical and experimental studies on the proton transfer reactions have been carried out to enrich the information regarding the possible mechanisms of proton transfer, tautomeric equilibria, etc.<sup>4-6</sup> The influence of *p*-electron delocalization on the characteristics of hydrogen bond interaction has also been analyzed<sup>7</sup>. For example, the so-called resonance assisted hydrogen bond (RAHB) model introduced and described by Gilli and co-workers<sup>8</sup>. It was reported that in RAHB systems there are conjugated double and single bonds where *p*-electron delocalization enhances the strength of hydrogen bonding. Also, an important role of the inter- and intra-molecular proton transfer has been demonstrated in all fields of molecular recognition<sup>9</sup> and association<sup>10</sup>.

3,6-Diimino-1,4-cyclohexadiene-1,4-diamine (DCD) is an organic compound which has two intramolecular hydrogens between the amino and imino groups for proton transfer (Fig. 1a). So far, the extensive studies have been focused on the proton transfer of DCD and its derivatives<sup>11-16</sup>. Holloway *et al.*<sup>11</sup> for the first time investigated the process of proton transfer of DCD at semiempirical and *ab initio* calculation levels.

Limbach *et al.*<sup>12</sup> had previously analyzed kinetic and deuterium isotope effects of DCD. In addition, the study of the intramolecular hydrogen-atom migration of DCD by ultraviolet radiation was reported<sup>13</sup>. In an

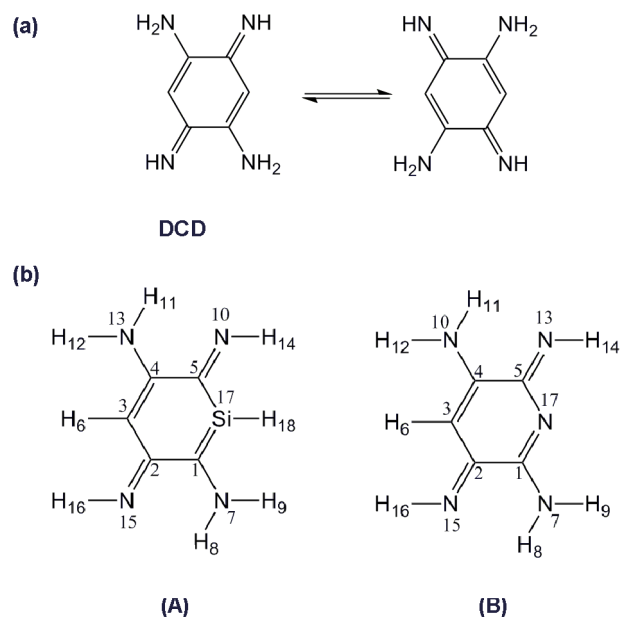


Fig. 1 – (a) The proton transfer process of 3,6-dihydro-3,6-diimino-1,4-cyclohexadiene-1,4-diamine (DCD), and, (b) structures of compounds (A) and (B).

other study, the proton transfer in azophenine, which is derivative from DCD, was studied by Rumpel *et al.*<sup>14,15</sup>, who suggested a stepwise single hydrogen atom transfer. In our previous study, we reported the effect of two similar heteroatoms (B, N, Si, P) on the proton transfer of DCD at DFT (B3LYP) level of theory<sup>16</sup>. To further our understanding of the process, herein, the effect of one heteroatom (silicon and nitrogen) on the proton transfer process in 3,6-dihydro-3,6-diiminosilene-2,5-diamine (A) and 3,6-dihydro-3,6-diiminopyridine-2,5-diamine (B), has been investigated (Fig. 1b). Since these compounds are asymmetric, the mechanisms of their proton transfer were different than that in DCD.

Previous studies<sup>17,18</sup> have shown that the density functional theory (DFT) studies are an alternative to *ab initio* method since DFT methods include a part of electron correlation effects (electrons in a molecular system react to each other's motion and attempt to keep out of one another's way) in their model. Moreover, molecular properties calculated with the DFT methods are in excellent agreement with the available experimental data for the systems containing the hydrogen bonding<sup>19-20</sup>. Thus, we used this method for analysing the proton transfer process in compounds (A) and (B).

The term "aromaticity" has the significant importance in organic chemistry because it is very useful in the rationalization of the structure, stability, and reactivity of many molecules. In particular, the degree of aromaticity in the heteroaromatic compounds is important since it helps in understanding the reactivity and their properties. In this study, we aim to study aromaticity of compounds (A) and (B) by the nucleus independent chemical shift (NICS) technique<sup>21</sup>. Studies have demonstrated that NICS is a useful indicator of aromaticity that usually correlates well with the other energetic, structural, and magnetic criteria for aromaticity.

### Methodology

The optimizations of all geometries have been carried out using density functional theory (DFT). One hybrid functional of the DFT method, which consists of the Becke's three parameters exact exchange functional (B3)<sup>22</sup> combined with the nonlocal gradient corrected correlation functional of Lee-Yang-Parr (LYP)<sup>23</sup> (B3LYP) has been used. The B3LYP calculations with the split valence 6-31+G(d,p) basis set were used<sup>23,24</sup>. The harmonic vibrational frequency calculations were performed for

all optimized species at the B3LYP/6-31+G(d,p) level to characterize the optimized stationary points as minima and to evaluate the corresponding zero-point vibrational energies. NICS values were obtained by calculating absolute NMR shielding at ring center (NICS(0)) and at 1.0 Å above the ring center (NICS(1)) at the B<sub>3</sub>LYP/6-311+G (2d,p) level of theory by using the Gauge-Independent Atomic Orbital (GIAO) method<sup>16,25,26</sup>. All calculations were performed by Gaussian 98 program package<sup>27</sup>.

## Results and Discussion

### Energy calculations

The pathways of proton transfer of the compounds (A) and (B) are shown in Fig. 2. According to Fig. 2, two mechanisms, i.e., stepwise (TS<sub>1</sub>) and concerted (TS<sub>2</sub>), are suggested for the proton transfer since these compounds have two intramolecular hydrogen bonds between the amino and imino groups. In stepwise mechanism, two pathways are feasible for proton transfer since they have the different resonance sides, the N-C-C-C-N side for pathway (1) and N-C-X-C-N (X= Si-H or N) side for pathway (2). In pathway (1), the resonance of GS structure from N-C-C-C-N side results in GS<sub>a</sub> structure, which can transfer an amine hydrogen atom to the imine nitrogen atom through TS<sub>1a</sub>. After the first transfer, the intermediate structures (Int<sub>a</sub>) produced can transfer the second proton by passing through TS'<sub>1a</sub> which is equal energetically to TS<sub>1a</sub>. Pathway (2) is similar to pathway (1) with the exception of the resonance from N-C-X-C-N side which results in GS<sub>b</sub>, TS<sub>1b</sub>, Int<sub>b</sub> and TS'<sub>1b</sub> structures, respectively which are energetically different from GS<sub>a</sub>, TS<sub>1a</sub>, Int<sub>a</sub> and TS'<sub>1a</sub> of pathway (1). In fact, the stepwise mechanism proceeds via two transition states (TS<sub>1a</sub> and TS'<sub>1a</sub> or TS<sub>1b</sub> and TS'<sub>1b</sub>) and one intermediate (Int<sub>a</sub> or Int<sub>b</sub>). In addition, the concerted (TS<sub>2</sub>) mechanism involves the simultaneous transfer of both protons in a single step (Fig. 2). The total energies of the structures at DFT level of theory are listed in Table 1. Also, the energy diagram of the zero point corrected energy for concerted and stepwise mechanisms of the compounds (A) and (B) at B3LYP/6-31+G (d,p) level of theory are presented in Figs 3 and 4. As can be seen in Fig. 3, the calculated relative energies of TS<sub>1a</sub>, TS<sub>1b</sub> and TS<sub>2</sub> for the compound (A) were 14.5, 18.43, and 26.37 kcal/mol, respectively. The corresponding values for compound (B) were 16.38, 16.71 and 27.2 kcal/mol, respectively (Fig. 4). In a previous study,

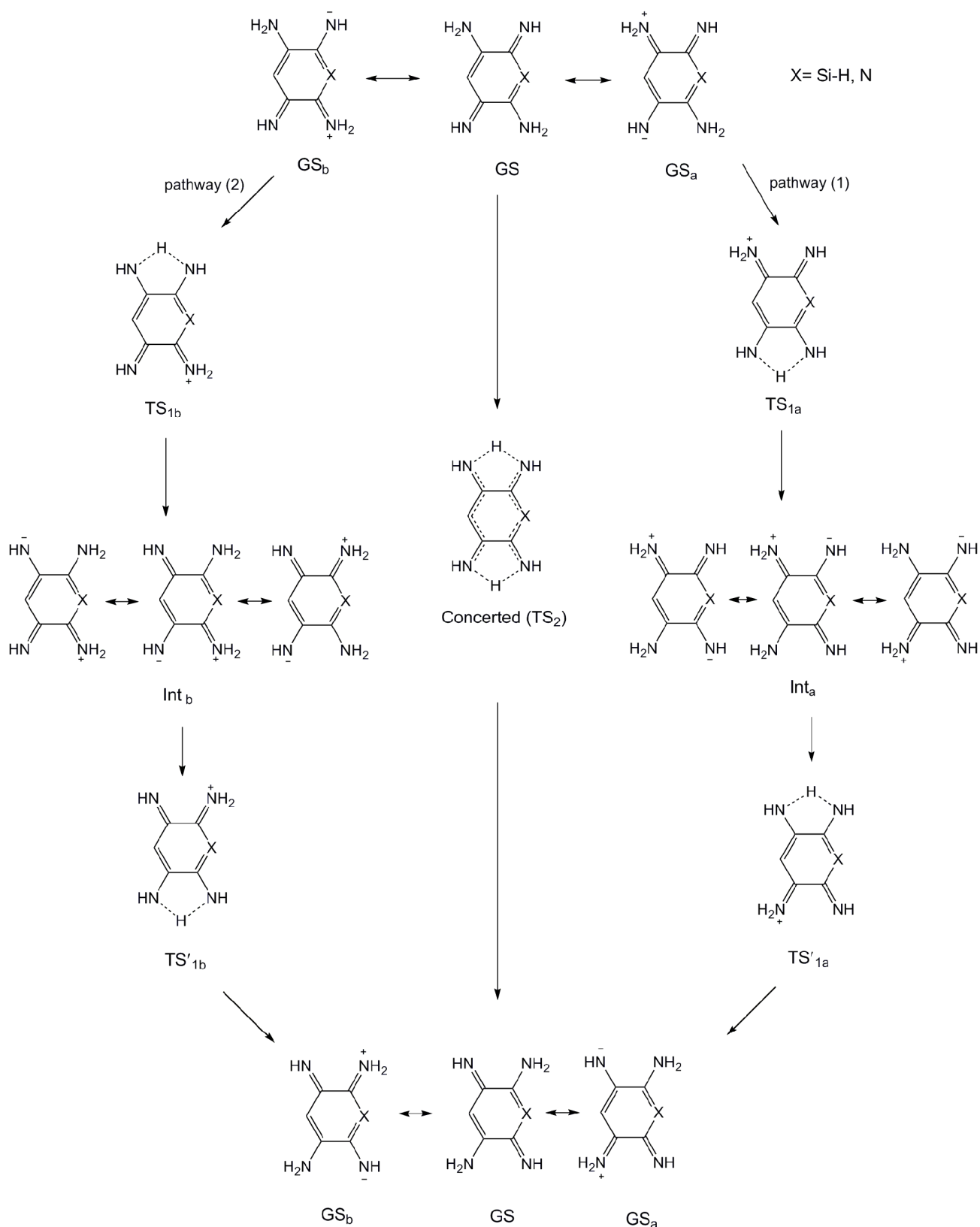


Fig. 2 – The stepwise and concerted mechanisms of the compounds (A) and (B).

Table 1 – The obtained total energy, relative energy and zero point vibrational energy (ZPVE) for intramolecular proton transfer of compounds (A) and (B) at B3LYP/6-31+G(d,p) level

| Comp. | Energies                    | GS <sub>0</sub> | GS          | TS <sub>1a</sub> = TS' <sub>1a</sub> | TS <sub>1b</sub> = TS' <sub>1b</sub> | Int <sub>a</sub> | Int <sub>b</sub> | TS <sub>2</sub> |
|-------|-----------------------------|-----------------|-------------|--------------------------------------|--------------------------------------|------------------|------------------|-----------------|
| A     | Total energy (hartree)      | -703.809488     | -703.808344 | -703.781432                          | -703.775137                          | -703.791127      | -703.780010      | -703.758521     |
|       | ZPVE (kcal/mol)             | 84.70483        | 84.12477    | 81.60302                             | 81.58214                             | 84.37236         | 84.18028         | 79.09176        |
|       | E <sub>rel</sub> (kcal/mol) | 0               | 0.138       | 14.5                                 | 18.43                                | 11.19            | 17.97            | 26.37           |
| B     | Total energy (hartree)      |                 | -468.534638 | -468.504345                          | -468.503974                          | -468.516351      | -468.515865      | -468.483135     |
|       | ZPVE (kcal/mol)             |                 | 83.15485    | 80.53048                             | 80.61884                             | 83.27566         | 83.38201         | 77.85368        |
|       | E <sub>rel</sub> (kcal/mol) |                 | 0           | 16.38                                | 16.71                                | 11.60            | 12.01            | 27.02           |

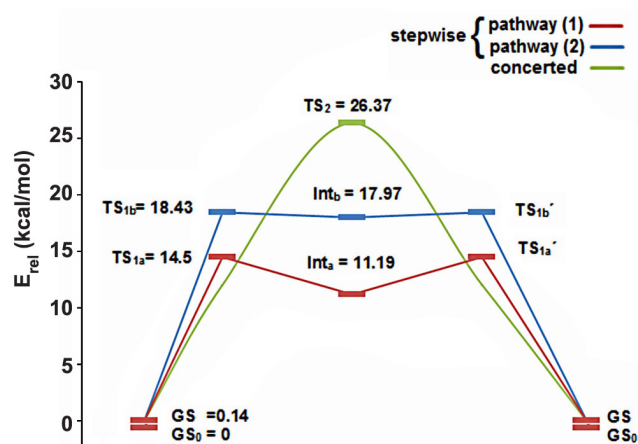


Fig. 3 – The diagram of the relative energy of the proton transfer process of the compound (A) at B3LYP/6-31+G (d,p) level of theory.

we have found that DCD has only one pathway for proton transfer in stepwise mechanism since the two pathways for resonance were similar<sup>16</sup>. These results show that the stepwise mechanism is more favorable than the concerted one in both compounds since the stepwise mechanism has a lower energy barrier than the concerted mechanism.

In compound (A), the presence of silicon atom in the ring causes the increase in energy difference between the two stepwise pathways. The results show that there are two structures, GS<sub>0</sub> and GS, for the ground state of compound (A) (Fig. 3). The energy difference of the two structures is very small (0.14 kcal/mol). However, the more stable structure is GS<sub>0</sub> which is non-planar unlike the GS structure, which is flat. In addition, no imaginary frequencies were found for GS<sub>0</sub>, which proves the energy minimum on the potential energy surface. For other optimized species, such as GS<sub>1</sub>, Int, TS<sub>1</sub> and TS<sub>2</sub>, imaginary frequencies 1, 1, 2 and 3, respectively

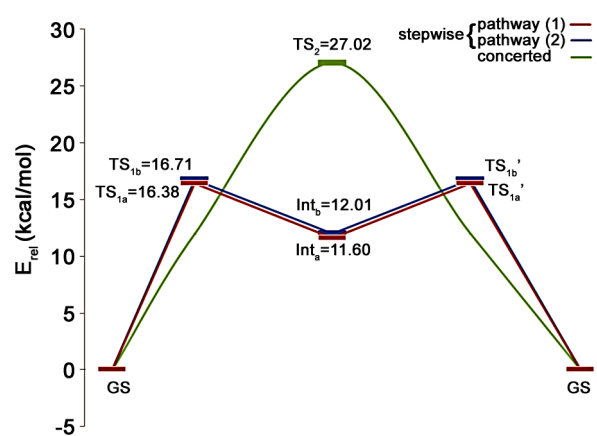


Fig. 4 – The diagram of the relative energy of the proton transfer process of the compound (B) at B3LYP/6-31+G (d,p) level of theory.

were found. The delocalization of  $\pi$ -electrons for proton transfer of H<sub>11</sub> in pathway (2), TS<sub>1b</sub>, requires 4 kcal/mol higher energy than proton transfer of H<sub>8</sub> of pathway (1), TS<sub>1a</sub>. In addition, the Int<sub>b</sub> structure is about 6.8 kcal/mol more unstable than Int<sub>a</sub>. The energy increase can be related to the large size of silicon atom, longer bond length of Si-C relative to C-C bond and using 3p orbital of silicon versus 2p orbital of carbon atom in the resonance. Hence, in the pathway (2) the resonance process in the silicon side of the ring hardly occurs and follows the energy increase for the TS<sub>1b</sub> and Int<sub>b</sub> structures. The obtained results for compound (B) were similar to those of DCD<sup>16</sup>. The energy difference between two stepwise pathways was very little (0.33 kcal/mol) and their energies were almost the same (16.71  $\approx$  16.38) (Fig. 4). In addition, energy difference between TS<sub>1a</sub> with Int<sub>a</sub> and TS<sub>1b</sub> with Int<sub>b</sub> structures was also approximately the same (4.7 kcal/mol). These values can be related to involvement of 2p orbitals of nitrogen and carbon

atoms in the resonance process as compared to  $3p$  orbital of silicon. In fact, the similarity of the C-N and C=N bonds, which cause better resonance, improves the proton transfer process that follows the energy decrease between  $TS_{1a}$  and  $TS_{1b}$  structures as compared to those of compound (A). In addition, imaginary frequencies for GS and Int,  $TS_1$  and  $TS_2$  structures were found to be 0, 1 and 2, respectively.

#### Structural parameters

The optimized geometrical structures of proton transfer process of the compound (A) are shown in Fig. 5. The  $GS_0$  structure, which has two intramolecular hydrogen bonds between the amino and imino groups, is non-planar, as the  $H_{18}$  is  $\sim 43^\circ$  out of the ring. Other structures are planar within  $1-2^\circ$ . The calculated bond lengths are listed in Table S1 (Supplementary Data); the numbering of atoms is as given in Fig. 5. The lengths of the  $C_1-C_2$  and  $C_4-C_5$  bonds for all structures are in the range  $1.502-1.550 \text{ \AA}$  suggesting single bond character, while those of  $C_2-C_3$  and  $C_3-C_4$  are in the range of  $1.367-1.463 \text{ \AA}$ , and those for  $C_1-Si$  and  $C_5-Si$  in the range of  $1.758-1.883 \text{ \AA}$ ,

are shorter than the C-C and C-Si single bonds, respectively. Similarly, the  $C_2-N_{15}$  and  $C_5-N_{13}$  bonds ( $1.292-1.332 \text{ \AA}$ ) and  $C_4-N_{10}$  and  $C_1-N_7$  ( $1.314-1.365 \text{ \AA}$ ) are shorter than the C-N single bonds.

Figure 6 shows the optimized structures of the compound (B). The calculated bond lengths for compound (B) are listed in Table S2 (Supplementary Data); the numbering of atoms is as given in Fig. 6. In compound (B), the bond lengths of the  $C_1-C_2$  and  $C_4-C_5$  for all structures show single-bond character, while those of  $C_2-C_3$  and  $C_3-C_4$ ,  $C_1-N_{17}$  and  $C_5-N_{17}$  are shorter than the single C-C and C-N bonds by  $\approx 0.1 \text{ \AA}$ , respectively. In addition, the  $C_1-N_7$  and  $C_4-N_{10}$  bonds ( $1.302-1.352 \text{ \AA}$ ) and  $C_2-N_{15}$  and  $C_5-N_{13}$  ( $1.287-1.328 \text{ \AA}$ ) are shorter than the C-N single bonds. Also, all structures in proton transfer process of compound (B) were planar. These comparisons suggest that the  $\pi$ -conjugation system in both compounds are separated into two parts; the  $N_{10}-C_4-C_3-C_2-N_{15}$  part and  $N_{13}-C_5-X_{17}-C_1-N_7$  ( $X = Si-H$  or  $N$ ) part. Bond and dihedral angles of compounds (A) and (B) are presented in Table S3-S6 (Supplementary Data).

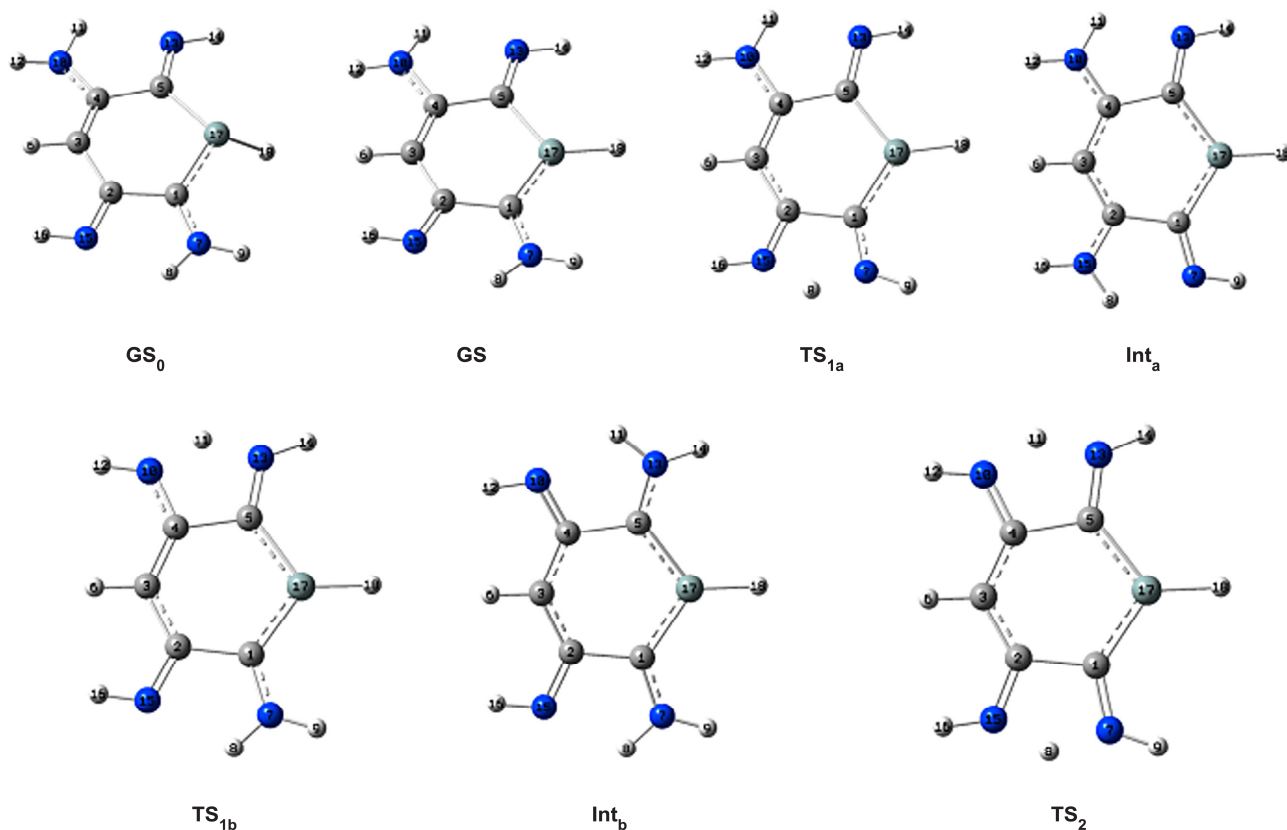


Fig. 5 – The optimized geometrical structures of proton transfer process of the compound (A).

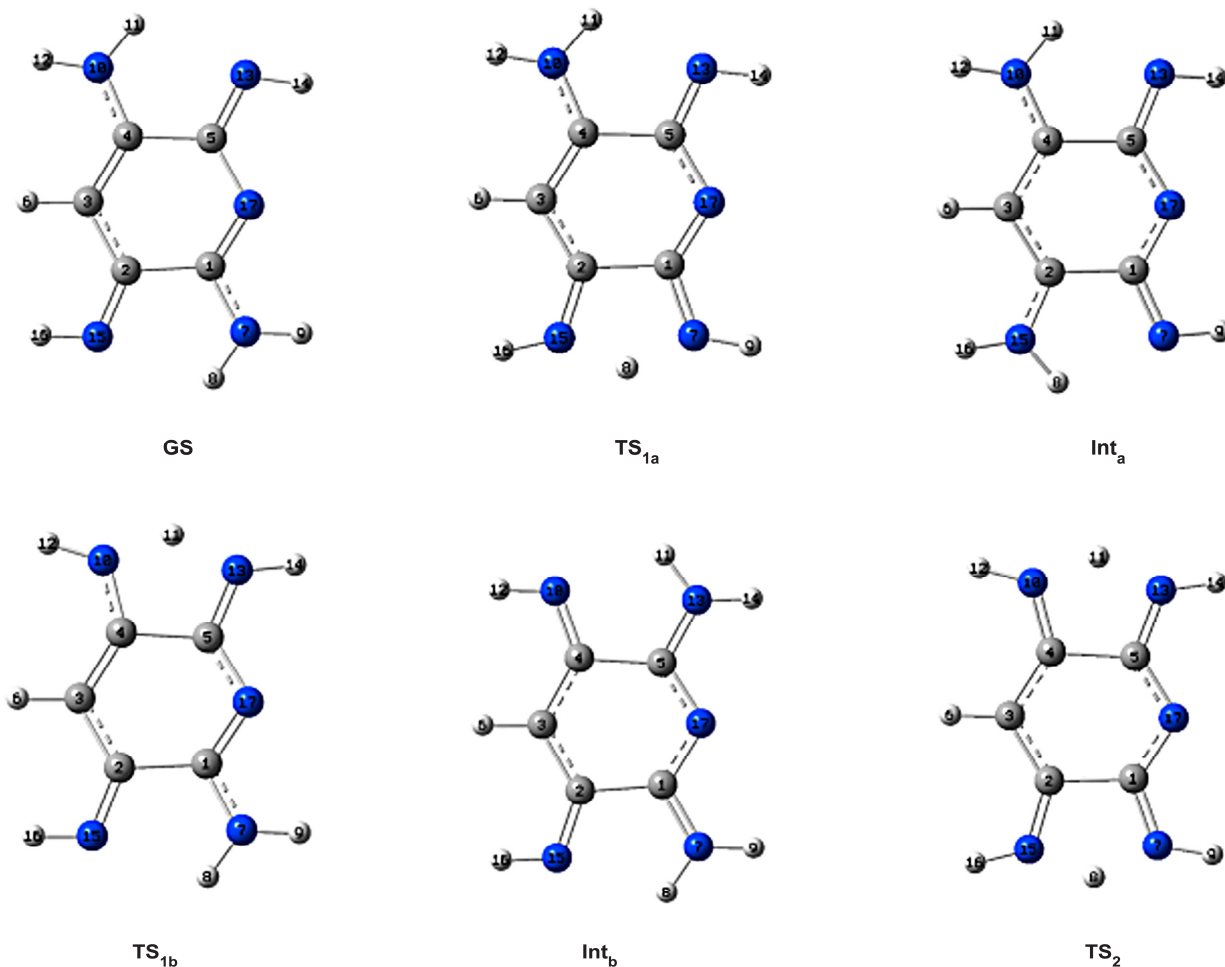


Fig. 6 – The optimized geometrical structures of proton transfer process of the compound (B).

#### Variance of Mulliken charge

Tables S7 and S8 (Supplementary Data) show the Mulliken charge population on all the atoms for both compounds. The data indicate that the charge on the labile hydrogen and nitrogen increase distinctively in the transition state. In other words, the proton transfer causes the separation of charge for both compounds. According to Table S7 (see Supplementary Data), the charge analysis of the compound (A) shows that the net atomic charge of the H atom that is transferred increases along the process from 0.348 for GS<sub>0</sub> to 0.400 for TS<sub>1a</sub> and from 0.337 for GS<sub>0</sub> to 0.407 for TS<sub>1b</sub>. Also, the charge population of the H<sub>8</sub> and H<sub>11</sub> is found to be 0.408 for TS<sub>2</sub>. Due to an increase of polarity of the formed bond, the reaction shows a certain degree of proton transfer character. The net negative charge on the N<sub>7</sub> atom is -0.451 for GS<sub>0</sub> and -0.528 for TS<sub>1a</sub>, that on the N<sub>15</sub> atom is -0.542 for GS<sub>0</sub> and -0.5998 for TS<sub>1a</sub>, for the N<sub>10</sub> atom it is -0.603 for

GS<sub>0</sub> and -0.707 for TS<sub>1b</sub>, and for the N<sub>13</sub> atom it is -0.409 for GS<sub>0</sub> and -0.440 for TS<sub>1b</sub>. The net negative charges of these nitrogen atoms increase during the proton transfer (GS<sub>0</sub> → TS). On this basis, it can be seen that most of the negative charges are localized on nitrogen atoms for both fragments, and most of the positive charges are populated on hydrogen atoms attached to nitrogen atoms. In fact, the highest values of the positive and negative charges in TS structures are distributed on the transferred hydrogen and nitrogen atoms, respectively. In compound (B), (Table S8, Supplementary Data), the charge population of H<sub>8</sub> is 0.346 for GS, 0.406 for TS<sub>1a</sub>, and 0.409 for TS<sub>2</sub> and that of H<sub>11</sub> is 0.346 for GS, 0.409 for TS<sub>1b</sub> and 0.409 for TS<sub>2</sub>. These values indicate that the charge on H<sub>8</sub> and H<sub>11</sub> increases during the proton transfer (GS → TS), which induces proton transfer character. In the transition states, the charge population on the N<sub>7</sub> is -0.615 for TS<sub>1a</sub>

Table 2 – NICS values (ppm) calculated at the ring center and 1 Å above at B3LYP/6-311+G(2d,p) level

| Comp. | NICS    | GS <sub>0</sub> | GS      | TS <sub>1a</sub> | Int <sub>a</sub> | TS <sub>1b</sub> | Int <sub>b</sub> | TS <sub>2</sub> |
|-------|---------|-----------------|---------|------------------|------------------|------------------|------------------|-----------------|
| A     | NICS(0) | 2.2785          | 1.4754  | 5.4133           | 13.0794          | 4.1836           | 4.6100           | 6.7602          |
|       | NICS(1) | 0.0436          | 0.6661  | 4.0702           | 11.5592          | 2.8953           | 3.6629           | 4.9886          |
| B     | NICS(0) |                 | 4.1351  | 5.2250           | 3.4591           | 5.7870           | 5.3330           | 6.6990          |
|       | NICS(1) |                 | -0.2638 | 0.3628           | -1.0510          | 0.7592           | 0.5353           | 1.2978          |

and -0.580 for TS<sub>2</sub> and that on the N<sub>15</sub>, it is -0.667 for TS<sub>1a</sub> and -0.698 for TS<sub>2</sub>, while these values for N<sub>7</sub> and N<sub>15</sub> are -0.553 and -0.608 in the GS structure, which shows that the net charge on the nitrogen atoms increase along the process. Also, similar results for the N<sub>10</sub> and N<sub>13</sub> in TS<sub>1b</sub> and TS<sub>2</sub> structures were obtained. In the process of GS to TS (GS → TS), the negative charge on the C<sub>3</sub> decreases which can be related to the delocalization of  $\pi$ -electrons in the proton transfer process. These results show that electrons are redistributed after the proton transfer.

#### Aromaticity

To calculate aromaticity of compounds (A) and (B), NICS criterion proposed by Schleyer *et al.*<sup>21</sup> has been used. This method is based on the negative value of the absolute shielding observed at a ring center of the system, usually above the ring center. Hence, rings with large negative NICS values are considered aromatic (diatropic ring current) and are the best for electron delocalization. Non-aromatic species have NICS values close to zero and the positive NICS values are indicative of antiaromaticity (paratropic ring current). NICS is usually computed at ring centers (NICS (0)) and 1 Å above/below the molecular plane (NICS (1)). NICS (1) essentially reflects  $\pi$  effects and is a better indicator of the ring current than the value at the center, because at 1 Å, the effects of the local  $\sigma$ -bonding contributions are diminished<sup>28-30</sup>. In other words, the obtained NICS (1) values are considered to improve the reflection of the  $\pi$ -electron effects and therefore, they are probably an even better descriptor of aromaticity than NICS (0). The NICS values obtained using the GIAO procedure at the B3LYP/6-311+G(2d,p) level are given in Table 2. As can be seen in Table 2, the NICS values (NICS (0) and NICS (1)) of all structures are almost the same for compound (A), while these values significantly differ from each other for compound (B). This indicates that compound (B) inclines towards higher resonance than compound (A). In compound (A), due to the 3p orbital of the silicon atom in the resonance (all structures), has a slight tendency for

proton transfer as compared to compound (B) which results in increase of the energy barrier. Hence, the difference of NICS values (NICS (0) and NICS (1)) in compound (A) is less. These values show that in most of the structures, the ring has antiaromatic properties, in particular in compound (A), which causes bond fixation in the ring and the ring avoids involvement in resonance, while NICS (1) values of GS and Int<sub>a</sub> structures of compound (B) show slight aromatic properties. Overall, the positive values of NICS for compound (A) indicate that the presence of silicon atom in the ring causes increase of bond length (C-Si-C). In addition, the existence of the different bonds (N-C-Si-C-N) and also use of 3p orbital of silicon atom in the resonance pathways result in the decrease of electron delocalization in the compound (A) which follows the increase of energy barrier and anti-aromaticity properties in the proton transfer process. Compound (B) shows higher aromaticity than compound (A), which can be related to the similarity of the bonds (C-N, C=N) and involvement of 2p orbitals (nitrogen and carbon) in the resonance. Therefore, the delocalization of  $\pi$ -electrons is higher than in compound (A), which is also confirmed by the NICS values.

#### Conclusions

The results obtained for proton transfer of compounds (A) and (B) showed that the stepwise mechanism is preferred to the concerted mechanism in both compounds. Also, due to the similarity of bond lengths in compound (B), the energy barriers for proton transfer in pathways (1) and (2) were almost similar to each other, while pathway (1) was favorable for compound (A). In addition, NICS results showed that compound (B) is more aromatic than compound (A) in the proton transfer process.

#### Supplementary Data

Supplementary data associated with this article, i.e., Tables S1-S8, are available in the electronic form at [http://www.niscair.res.in/jinfo/ijca/IJCA\\_55A\(05\)529-536\\_SupplData.pdf](http://www.niscair.res.in/jinfo/ijca/IJCA_55A(05)529-536_SupplData.pdf).

**References**

- 1 Coll M, Frau J, Vilanova B, Llinas A, Donoso J & Munoz F, *Int J Chem*, 2 (1999) 3.
- 2 Madeja F & Havenith M, *J Chem Phys*, 117 (2002) 7162.
- 3 Alavi S L D, *J Chem Phys*, 117 (2002) 2599.
- 4 Kulhanek P, Schlag E W & Koca J, *J Am Chem Soc*, 125 (2003) 13678.
- 5 Li P & Bu Y, *J Phys Chem A*, 108 (2004) 10288.
- 6 Sun Y, Li H, Liang W & Han S, *J Phys Chem B*, 109 (2005) 5919.
- 7 Sobczyk L, Grabowski S J & Krygowski T M, *Chem Rev*, 105 (2005) 3513.
- 8 Gilli G, Belluci F, Ferretti V & Bertolesi V, *J Am Chem Soc*, 111 (1989) 1023.
- 9 Babine R E & Bender S L, *Chem Rev*, 97 (1997) 1359.
- 10 Tolosa S, Hidalgo A & Sansó n J A, *Chem Phys*, 255 (2000) 73.
- 11 Holloway M K, Reynolds C H & Merz Jr K M, *J Am Chem Soc*, 111 (1989) 3466.
- 12 Limbach H, Hennig J, Gerritzen D & Rumpel H, *J Chem Soc Faraday Discuss*, 74 (1982) 229.
- 13 Ujike K, Kudoh S & Nakata M, *Chem Phys Lett*, 409 (2005) 52.
- 14 Rumpel H, Limbach H H & Zachmann G, *J Phys Chem*, 93 (1989) 1812.
- 15 Rumpel H & Limbach H H, *J Am Chem Soc*, 111 (1989) 5429.
- 16 Tahermansouri H, Moradi S & Sayyadi R, *Indian J Chem*, 50A (2011) 180.
- 17 Jursic B S, *Int J Quantum Chem*, 57 (1996) 213.
- 18 Bytheway I, Bacskey G B & Hush NS, *J Phys Chem*, 100 (1996) 6023.
- 19 Martin J M L & Alsenoy C, *J Phys Chem*, 100 (1996) 6973.
- 20 Lampert H, Mikenda W & Karpfen A, *J Phys Chem*, 100 (1996) 7418.
- 21 Schleyer P v R, Maerker C, Dransfeld A, Jiao H & Hommes N J R v E, *J Am Chem Soc*, 118 (1996) 6317.
- 22 Becke A D, *J Phys Rev A*, 38 (1988) 3098.
- 23 Lee C, Yang W & Parr R G, *J Phys Rev B*, 37 (1988) 785.
- 24 Becke A D, *J Chem Phys*, 98 (1993) 5648.
- 25 Keith T A & Bader R F W, *Chem Phys Lett*, 210 (1993) 223.
- 26 Cheeseman J R, Trucks G W, Keith T A & Frisch M J, *J Chem Phys*, 104 (1996) 5497.
- 27 *Gaussian 98, Rev. A7*, (Gaussian Inc, Pittsburgh, PA) 1998.
- 28 *Progress in Nuclear Magnetic Resonance Spectroscopy*, edited by P Lazzereti, J W Emsley & J L H Feeney, Sutcliffe, Vol. 36, (Elsevier, Amsterdam) 2000, p. 1.
- 29 Schleyer P v R, Manoharan M, Wang Z X, Kiran B, Jiao H J, Puchta R & Hommes N J R v E, *Org Lett*, 3 (2001) 2465.
- 30 Corminboeuf C, Heine T, Seifert G, Schleyer P v R & Weber J, *Phys Chem Chem Phys*, 6 (2004) 273.